Fibronectin Mediates Endothelial-to-Mesenchymal Transition in Retina Angiogenesis

Dan Liu,[1–3] Zhishang Meng,[3] Chen Jin,[4] Fang Chen,[5] Li Pu,[1,2] Ze Wu,[6] Qi Zeng,[7] Jing Luo,[3] and Wenyi Wu[1,2]

[1]Department of Ophthalmology, Hunan Key Laboratory of Ophthalmology, Xiangya Hospital, Central South University, Changsha, China
[2]National Clinical Research Center for Geriatric Disorders, Xiangya Hospital, Changsha, China
[3]Department of Ophthalmology, The Second Xiangya Hospital, Central South University, Changsha, China
[4]Department of Neurosurgery, Xiangya Hospital, Central South University, Changsha, China
[5]Huan Key Laboratory of Molecular Precision Medicine, Xiangya Hospital and Hunan Key Laboratory of Medical Genetics, School of Life Sciences, Central South University, Changsha, China
[6]Department of Pathology, Xiangya Hospital, Central South University, Changsha, China
[7]Hunan Provincial People's Hospital, The First Affiliated Hospital of Hunan Normal University, Hunan, China

Correspondence: Jing Luo, 139 Renming Street, Furong, Changsha, Hunan, China; luojing001@csu.edu.cn.
Wenyi Wu, 87 Xiangya Street, Kaifu, Changsha, Hunan, China; wenyi_wu@csu.edu.cn.

DL, ZM, and CJ contributed equally to this work.

Received: November 22, 2024
Accepted: February 9, 2025
Published: March 5, 2025

Citation: Liu D, Meng Z, Jin C, et al. Fibronectin mediates endothelial-to-mesenchymal transition in retina angiogenesis. *Invest Ophthalmol Vis Sci.* 2025;66(3):10. https://doi.org/10.1167/iovs.66.3.10

Purpose. The purpose of this study was to investigate the role of endothelial-mesenchymal transition (EndoMT) in pathological retinal angiogenesis and identify key molecular mediators in retina angiogenesis.

Methods. RNA sequencing (RNA-seq) was performed on retinal tissue from an oxygen-induced retinopathy (OIR) mouse model to analyze gene expression patterns. The Gene Set Enrichment Analysis was used to examine the correlation between epithelial-mesenchymal transition (EMT) and angiogenesis gene sets. Fibronectin (*FN1*) expression was evaluated in endothelial cells, and its function was assessed through siRNA-mediated knockdown in both in vitro angiogenesis assays and the OIR model.

Results. EndoMT occurred early in retinal angiogenesis development, with significant correlation between EMT and angiogenesis gene sets. *FN1* was identified as the most significantly upregulated EMT-related gene in endothelial cells. The siRNA-mediated inhibition of fibronectin effectively prevented VEGF-induced angiogenesis in vitro and reduced pathological angiogenesis in the OIR model.

Conclusions. EndoMT is a crucial early event in pathological retinal angiogenesis, with fibronectin serving as a key mediator. Targeting fibronectin may provide a novel therapeutic strategy that could synergize with anti-VEGF treatments to more effectively treat pathological angiogenesis in diabetic retinopathy (DR) and retinopathy of prematurity (ROP), particularly in cases of poor response to anti-VEGF therapy alone.

Keywords: endothelial dysfunction, angiogenesis, fibrosis, VEGF signaling, endothelial-mesenchymal transition (EndoMT)

The eye provides a sound model system to investigate the molecular signals in angiogenesis. The study of ocular angiogenesis has enormous clinical significance because, in developed countries, retinal neovascularization resulting from diabetic retinopathy (DR) is the most common cause of new blindness in young patients, and choroidal neovascularization (CNV) resulting from age-related macular degeneration (AMD) is the most common cause of severe vision loss in elderly patients. A detailed investigation uncovers that the progression of neovascularization followed by retinal fibrosis is the primary pathology of DR and retinopathy of prematurity (ROP).[1–3] Despite advancements in anti-VEGF therapy in treating proliferative diabetic retinopathy (PDR) and ROP over the last decade, non-response patients with antiangiogenic agents had increased, suggesting the involvement of alternative angiogenic mechanisms that do not solely rely on VEGFA ligands.[4] Thus, understanding the deep molecular mechanism of hypoxia-induced angiogenesis becomes imperative.

Oxygen-induced retinopathy (OIR) mice exhibit severe retinal microvascular malformations, and this model is the most widely used animal model to study neovascular mechanisms.[5] So, we applied the RNA-sequence (RNA-seq) to study the molecular mechanism of retina angiogenesis. Notably, the data unveil a significant elevation of fibronectin (*FN1*), including other epithelial-mesenchymal transition (EMT) markers in OIR, and *FN1* was the highest expression in the endothelial cells. This means that endothelial cells partially lose endothelial identity and acquire mesenchymal characteristics, or it might facilitate angiogenesis through a VEGFA-independent pathway. The outgrowth of fibrovascular epiretinal membranes at the vitreoretinal

interface in PDR or ROP might derive from ischemia-induced pathologic growth of new blood vessels accompanied by the expansion of the extracellular matrix (ECM). Thus, there must be a relation between fibrotic disorders and neovascularization.

Fibronectin (*FN1*) is a ubiquitous extracellular glycoprotein soluble in body fluids and insoluble in the ECM. It plays a significant role in many critical physiological processes, such as embryogenesis, wound healing, hemostasis, and thrombosis,[6] and includes an essential determinant of angiogenic activity through interaction with VEGF.[7] Moreover, it has been documented that endothelial-mesenchymal transition (EndoMT) facilitates angiogenesis through a fibronectin-rich matrix and promotes endothelial cell activation during monocyte recruitment.[8] Cell culture studies show that an fibronectin matrix promotes nuclear factor-κB (NF-κB) signaling and proinflammatory gene expression.[9] Despite the well-described role of fibronectin in endothelial activation and hemodynamic activation fibronectin expression,[10] the mechanisms regulating the *FN1* increase in hypoxia-induced retina angiogenesis remain largely unknown. During angiogenesis, the fibronectin that accumulates in the subendothelial matrix could transduce signaling by $\alpha5\beta1$ integrins on endothelial through PI3K/AKT and MAPK pathway, which promotes proliferation and migration.[11] Analysis of mRNA isolated from the retina in OIR shows that $\alpha5\beta1$ integrins and NF-κB activation (data not shown in the figures). We previously demonstrated that vitreous factors could increase fibronectin and promote endothelial cell proliferation,[12] but no other factors that activate fibronectin are known. In this study, we provide the role of fibronectin in angiogenesis and explore a potential drug to prevent its activity in the retina angiogenesis model. In conclusion, our results introduce a novel understanding of the concurrent occurrence of EndoMT alongside angiogenesis, highlighting the role of *FN1* in pathological retinal angiogenesis.

Materials and Methods

Primary Reagents and Cell Culture

Antibodies against Fibronectin, Vimentin, p-Akt, Akt, p-Erk, Erk, p-VEGFR2, and VEGFR2 were purchased from Cell Signaling Technology (Danvers, MA, USA). Antibodies against β-actin were purchased from Santa Cruz Biotechnology (Santa Cruz, CA, USA). Secondary horseradish peroxidase (HRP) antibodies-conjugated goat anti-rabbit IgG and anti-mouse IgG were purchased from Santa Cruz Biotechnology (Santa Cruz, CA, USA). Enhanced chemiluminescent substrate for detection of HRP was obtained from Thermo Fisher Scientific (Waltham, MA, USA). Primary human retinal microvascular endothelial cells (HRECs) were purchased from Cell Systems (Kirkland, WA, USA) and cultured and grown at 37°C with 5% CO_2 with endothelial growth medium (EGM)-2 kit (Lonza, Walkersville, MD, USA).

Preparation of RNA-Seq Samples and Data Analysis

TRIzol was used to extract total retinal RNA from retinal tissues, and cDNA libraries were sequenced by Novogene Co., Ltd. (Beijing, China) using an Illumina platform. Transcripts per million (TPM) normalized all RNA-seq data in our study.

Gene Set Enrichment Analysis, Gene Set Variation Analysis, and Differentially Expressed Genes Analysis

To explore the enriched differences of EMT and angiogenesis pathways and the inter-relationships between the healthy control and OIR groups, gene set enrichment analysis (GSEA) and gene set variation analysis (GSVA) were performed to calculate the gene signature scores using GSEA software[13] (version 4.3.2) and R package "GSVA"[14] in our RNA-seq data and other three data sets from the GEO database (GSE194176, GSE123945, and GSE158799).[15–17] The gmt files of the gene set used for the analysis were downloaded from the Molecular Signatures Database (MSigDB; https://www.gsea-msigdb.org/gsea/msigdb/) and are provided as Supplementary Table S1 in the additional information. Statistical significance was determined by normalized enrichment score (NES) > 1.0, P value < 0.05, and false discovery rate (FDR) < 0.25. Differential expression analysis on the three RNA-seq datasets was carried out using the "limma" R package; those genes that met $|\log \log2(\text{fold change})| > 1$ and adjusted P values < 0.05 were considered differentially expressed genes (DEGs). The results of GSVA were visualized as a heatmap using the R package "heatmap." The DEGs, GSEA, and Pearson correlation results among GSVA scores were visualized using Sangerbox software.

Survival and Gene Correlation Analysis

The cancer survival analysis and gene correlation studies were performed using the GEPIA web server (http://gepia.cancer-pku.cn/), which integrates The Cancer Genome Atlas (TCGA) and GTEx datasets. For survival analysis, the patients were divided into high and low FN1 expression groups using the median expression as the cutoff. For correlation analysis, Pearson correlation coefficients were calculated between *FN1* and selected genes involved in the VEGF/FGF pathways using the TCGA-GBM dataset. The correlation plots were generated using GEPIA2's correlation analysis tool within the website's instructions.

We downloaded the standardized pan-cancer dataset from the UCSC database (https://xenabrowser.net/): TCGA Pan-Cancer (PANCAN, N = 10535, G = 60499). From this dataset, we extracted the expression data of the ENSG00000115414 (*FN1*) gene across all samples. Additionally, we obtained high-quality TCGA survival data from a previously published Cell paper.[18] From this survival dataset, we removed samples with follow-up times shorter than 30 days.

We performed a log2 (x + 0.001) transformation on each expression value. Furthermore, we excluded cancer types with fewer than 10 samples. This resulted in a final dataset comprising 39 cancer types. The final dataset contains both expression data and corresponding overall survival information for all included samples.

siRNA Transfection

The non-target siRNA (NT siRNA) and *FN1*-siRNA were commercially obtained from APExBio company (Shanghai, China). The siRNAs were transfected into cells following the manufacturer's Lipofectamine 2000 protocol (Invitrogen). Quantitative PCR (qPCR) and Western blotting detected the silencing efficiency at 24 hours after transfection.

Investigative Ophthalmology & Visual Science

Cell Proliferation Assay

Using a cell counter, HRECs at a density of 2×10^4 cells in 24-well plates were estimated after 24 hours of continuous treatment with EGM-2 or VEGFA (50 ng/mL). At least three independent experiments were performed as described previously.

CCK-8 Assay

The proliferation of human umbilical vein endothelial cells (HUVECs) was examined using a CCK-8 kit according to the manufacturer's instructions. HUVECs were seeded into 96-well plates at the density of 2 × 103 cells per well with 100 µL of complete culture medium and cultured for 24 hours before reagents treatment. In the end, 10 µL of CCK-8 solution was added to each well and incubated for 1 hour. The absorbance at 450 nm was detected using a microplate reader.

Scratch-Wound Migration Assay

Migration was assessed with the scratch-wound assay[19] with minor modifications. One scratch was generated per well and imaged on a Zeiss microscope every 6 hours for 48 hours. Images were analyzed by measuring the number of pixels in the wound area using Adobe Photoshop and ImageJ software.[20]

Immunofluorescence

Embedded frozen eyes from the OIR model were prepared as described previously. Mouse eyes on slides or cultured HRECs were fixed in 3.7% formaldehyde/PBS for 10 minutes. Subsequently, the sections or cells were preincubated with 5% normal goat serum in 0.3% Triton X-100/PBS for 20 minutes and incubated with primary antibodies against FN1(1:100 dilution) (Cat. ab2413; Abcam, Cambridge, MA, USA), CD31 (cat:3528S; CST, Danvers, MA, USA) for 1 hour or a normal rabbit IgG. After 3 washes with PBS, the tissues and sections were incubated with fluorescently labeled secondary antibody DyLight 488 or 594 (Cat. DI-1549; Vector Laboratories, Burlingame, CA, USA; 1:500 dilution in blocking buffer) for 30 minutes. Following three washes with PBS, the slides were mounted with a mounting medium containing DAPI (solar cat: s2110) and photographed under a fluorescence microscope (Zeiss, ApoTome).

Statistical Analysis

Results are presented as mean ± SD. The Student's *t*-test was performed for comparisons between two groups, and 1-way ANOVA (Kruskal-Wallis test) was used for comparisons between multiple groups. A P value < 0.05 was considered significant.

Results

The Character of RNA-Seq in OIR

The murine model of OIR (Fig. 1a) has been used extensively to study retina angiogenesis in ROP and PDR. In this study, we utilize RNA-seq techniques to delve into the alterations in transcription and pinpoint a target associated with hypoxia-triggered retinal angiogenesis (see Fig. 1a). Our experimental group consists of OIR retinas collected at post-natal day 17 (p17) age, whereas control specimens comprise age-matched mice raised in normal oxygen conditions. Expectedly, a total of 938 differentially regulated genes (DRGs) emerge from the comparison of OIR retinas to p17 retinas, with 830 exhibiting upregulation and 108 displaying downregulation emerge from the comparison of OIR retinas to p17 retinas, with 830 showing upregulation and 108 displaying downregulation (Fig. 1b). To validate our model, we used a heatmap to visualize an angiogenesis-related gene set, confirming the efficacy of our angiogenesis model (Fig. 1c), The ridgeline plot showcases noteworthy distinctions in the distribution of genes like *vtn, vegfa*, and *app* between the two groups (Fig. 1d). Furthermore, examining EMT-related gene sets using a heatmap reveals substantial dissimilarity between OIR and control retinas (Supplementary Fig. S1a). The ridgeline plot is used to graphically represent the distribution of numeric variables tied to EMT genes, uncovering notable variations in genes such as *vim*, *sparc*, *fn1*, *col4a2*, and *col4a1* (Supplementary Fig. S1b).

Furthermore, enrichment and pathway analyses were performed using Gene Ontology (GO), Kyoto Encyclopedia of Genes and Genomes (KEGG), and Reactome pathways, respectively. The data show that GO enriched the DEGs in angiogenesis and extracellular matrix activity, and the 10 most significant terms in biological processes (BPs), molecular functions (MFs), and cellular components (CCs) are shown in Figure 1e. Moreover, exploring signaling pathways associated with differential gene enrichment was executed through KEGG and Reactome analyses. These analyses revealed that the most pronounced enrichment of DEGs occurred within PI3K/Akt-related pathways (Fig. 1f) and signaling pathways related to the organization of the extracellular matrix (Supplementary Fig. S2).

EMT Is Upregulated and Correlated With Angiogenesis

Retinal hypoxia is the stimulus for anomalous vessel proliferation and heightened microvascular permeability in conditions marked by ischemic retinopathies. During our investigations, we also observed an elevation in EMT during this progression, a finding supported by our sequence data and supplementary information from the GEO datasets. As shown in Figures 2a to 2c, GSEA revealed that gene sets associated with EMT and angiogenesis was significantly enriched in the OIR model group compared with the control group (see Fig. 2a). Specifically, nine distinct gene sets including HALLMARK EMT (NES = 1.4763, FDR = 0.0480), GOBP angiogenesis (NES = 1.4562, FDR = 0.0480), HALLMARK angiogenesis (NES = 1.3597, FDR = 0.1769), and six other of those related to angiogenesis in our RNA-seq data (see Fig. 2a).

Moreover, eight gene signatures include HALLMARK EMT (NES = 1.7505, FDR = 0.0530), GOBP sprouting angiogenesis (NES = 1.4056, FDR = 0.1254), and six other angiogenesis associated in the GSE194176 dataset (see Fig. 2b), and seven gene sets that include HALLMARK EMT (NES = 1.6135, FDR = 0.0093), GOBP positive regulation of sprouting angiogenesis (NES = 1.4144, FDR = 0.1088), and five other associated with angiogenesis in the GSE123945 dataset (see Fig. 2c). Subsequently, we performed GSVA to quantify EMT and angiogenesis scores for each sample in our dataset and GSE123945 (the complete results of the GSVA scores are

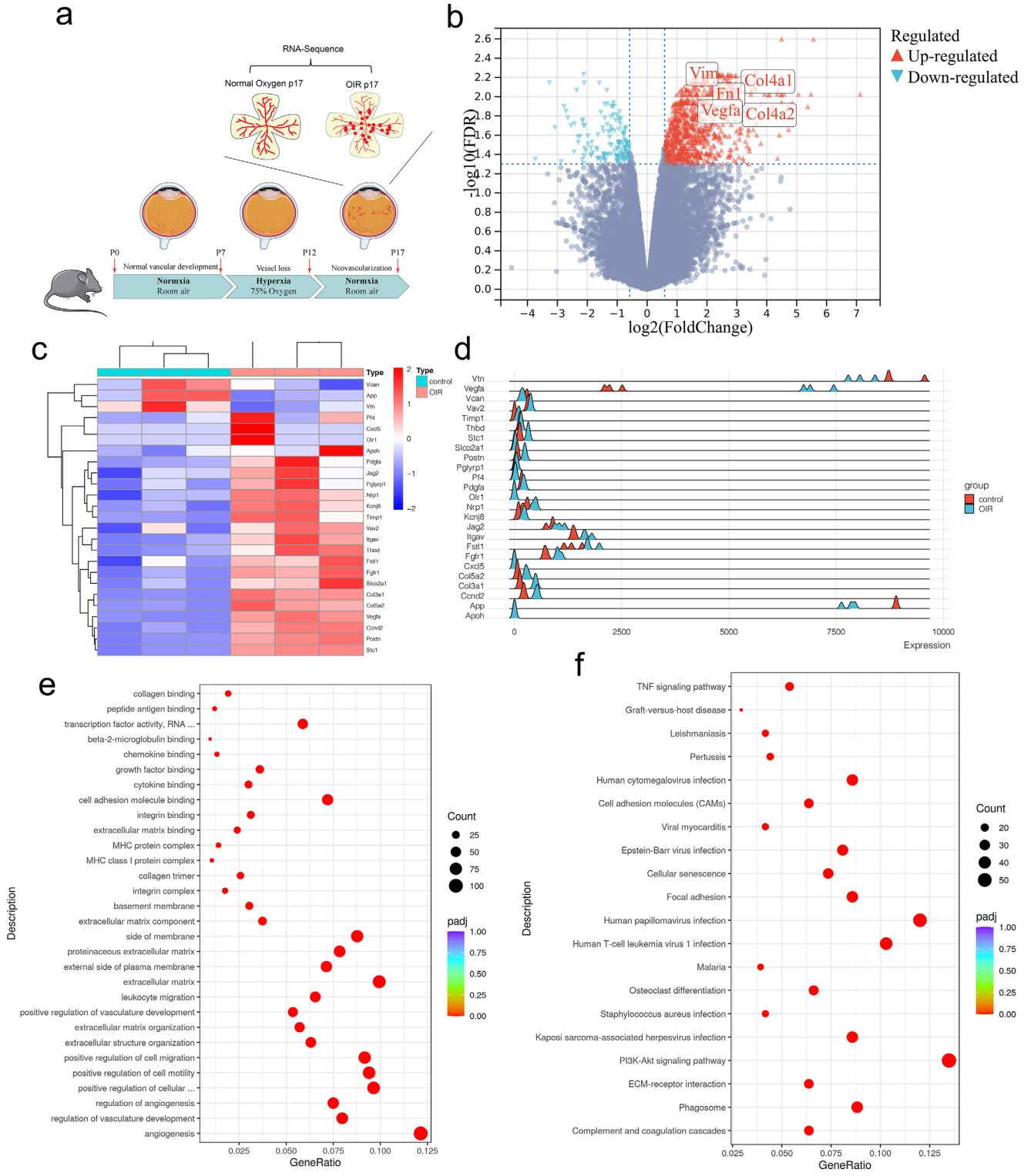

Figure 1. Experiment design and high-throughput sequencing of the retina from oxygen-induced retinopathy. (**a**) Schematic diagram of the OIR model. (**b**) The volcano plots showed 938 differential gene expressions (DGEs) between the P17 OIR model and the control group (FDR < 0.05, log2(fold change)| >1). (**c**) The heatmap shows the significant gene expression differences between the P17 OIR model and the control group in angiogenesis-related genes. (**d**) The ridgeline plot displays the angiogenesis-gene expression of each sample; *blue* and *red ridgelines* represent the P17 OIR model and the control group, respectively. (**e**) Enrichment of DRGs in GO database ($P < 0.05$, $q < 0.05$). (**f**) Enrichment of DRGs in the KEGG database ($P < 0.05$, $q < 0.05$).

Investigative Ophthalmology & Visual Science

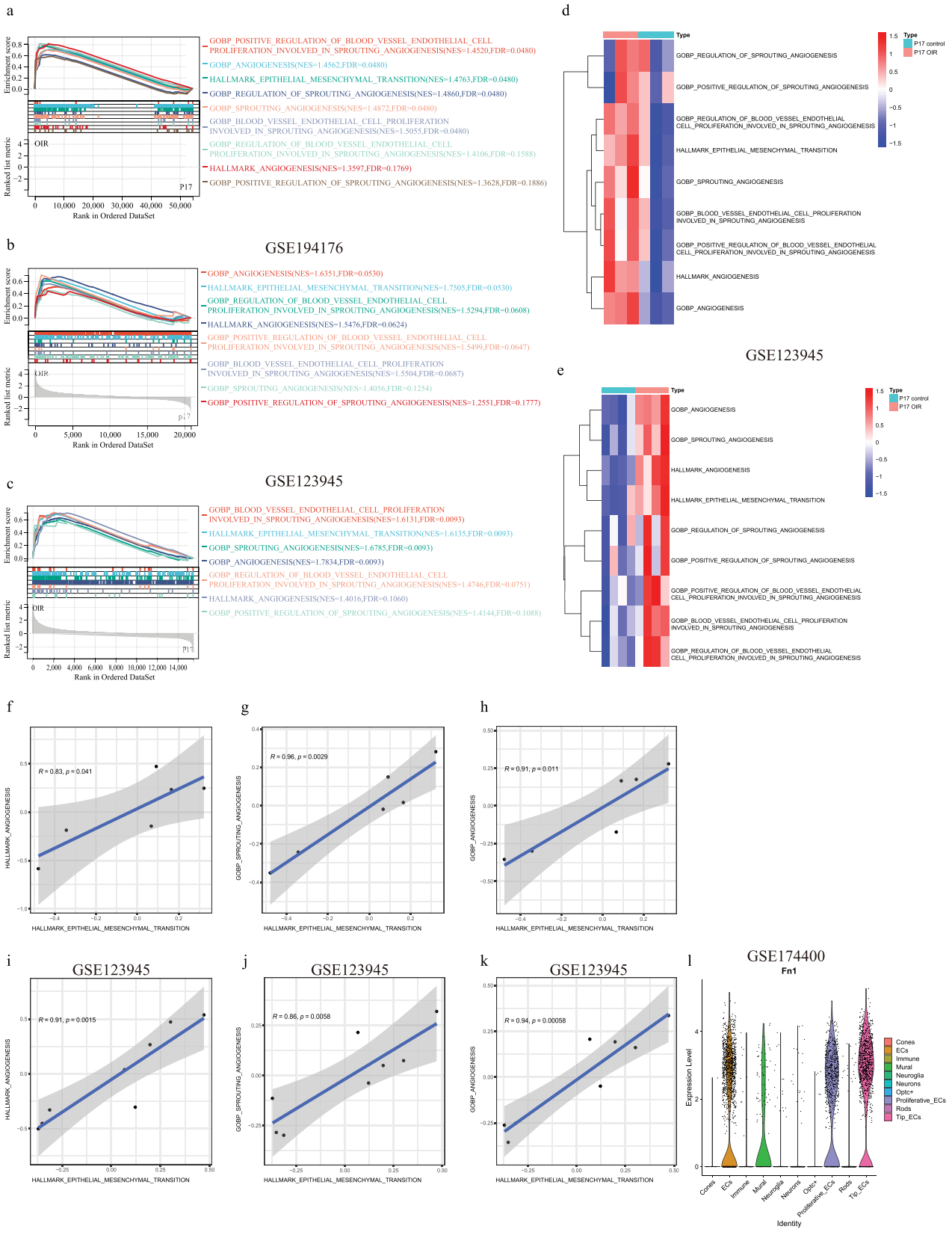

Figure 2. Transcriptomic analyses indicate EMT correlated with angiogenesis. (**a**) In the results of GSEA (GSEA analysis by CAMERA) using selected gene sets, each curve represents a gene set that significantly enriches the dataset. The colors of the curves correspond to the colors of the annotation given on the *right side*. (**b**) The GSEA plot of the top 8 ranked selected gene sets significantly enriches GSE194176. (**c**) The GSEA plot of the top 8 ranked selected gene sets significantly enriches GSE123945. (**d**) Hierarchical clustering heatmap of the GSVA enrichment scores for the nine gene sets. (**e**) GSVA enrichment scores for the 9 gene sets in GSE123945. (**f**) Scatter plots between HALLMARK epithelial-mesenchymal transition scores and hallmark angiogenesis ($R = 0.83$, $P = 0.041$). (**g**) Scatter plots between EMT and

Investigative Ophthalmology & Visual Science

GOBP-sprouting angiogenesis ($R = 0.96$, $P = 0.0029$). (**h**) Scatter plots between EMT and GOBP-angiogenesis ($R = 0.91$, $P = 0.011$). (**i**) Scatter plots between HALLMARK epithelial-mesenchymal transition scores and hallmark angiogenesis in GSE123945 ($R = 0.91$, $P = 0.0015$). (**j**) Scatter plots between EMT and GOBP-sprouting angiogenesis in GSE123945 ($R = 0.86$, $P = 0.0058$). (**k**) Scatter plots between EMT and GOBP-angiogenesis in GSE123945 ($R = 0.94$, $P = 0.00058$). (**l**) Single-cell sequence data form GSE174400, expression of *FN1* in different cell types from the OIR mouse model.

available in Supplementary Table S1), the resulting heatmap was displayed in Figure 2e, it was clear that there were significant differences between the control and OIR model groups in mice at P17 in both datasets. In Figures 2f to 2h, the Spearman correlation between the GSVA EMT and GSVA angiogenesis score is presented as a scatter plot. HALLMARK EMT scores are consistently positively correlated with three angiogenesis signature scores in our data (see Figs. 2f–h) and GSE123945 databases (Figs. 2i–k), including HALLMARK angiogenesis, GOBP sprouting angiogenesis, and GOBP angiogenesis.

More importantly, endothelial cells (ECs) undergo a comprehensive transformation known as an EndoMT, resulting in the development of an endothelial-derived mesenchymal phenotype within the context of OIR, as demonstrated in Figure 2l of the GSE174400 dataset).

FN1 Is One of the Most Significantly Increased Genes in OIR

Fibronectin is a glycoprotein with wide-ranging distribution within diverse cell structures, including the smooth muscle cell layer and vascular cell membrane. Its fundamental role is facilitating interactions between cells and the extracellular matrix, participating in crucial cellular processes such as adhesion, migration, growth, and differentiation. During the OIR sequence, we found that *FN1* was one of the most significantly upregulated genes during the angiogenesis phase of retinal development (see Fig. 1a). This heightened *FN1* expression was further validated via qPCR performed on OIR retinas, contrasting them against normal p17 retinas (Supplementary Fig. S3). A single-cell sequence from GSE150703 of the OIR model shows that *FN1* was highly expressed in endothelial cells and pericytes (Fig. 3a). To examine the precise localization of fibronectin, our attention focused on its expression within the OIR retina, particularly within endothelial cells. Through the application of immunohistochemical and immunofluorescence methodologies, we discerned an elevated presence of fibronectin within the vascularized OIR retina (Fig. 3b); this formal presence was particularly pronounced in pathological vessels (Fig. 3c) and tip cell (Fig. 3d). In contrast, fibronectin expression was notably absent in the vessels of the normal retina at P18 (see Fig. 3c).

FN1 Is a Biomarker Interacting With Tumor Vessels' VEGF and FGF Pathways

Glioblastomas are aggressive astrocytic brain tumors characterized by microvascular proliferation and an abnormal vasculature.[21] Fibronectin has been demonstrated to promote cell proliferation and migration in gastric cancer cell lines and predict a poor prognosis in glioblastoma.[22,23] Fibronectin can also predict poor prognosis and short survival in choroidal melanoma (Fig. 4a) and glioblastoma (Figs. 4b, 4c) in the TCGA dataset by using the GEPIA website.[24] The RNA expression rate of *FN1* in cancer compared with their control was seen in Supplementary Figure S4, and prognostic effects of *FN1* on pan-cancer are presented in a forest plot (Fig. 4d); the patients with high expression of *FN1* tended to have worse outcomes in 17 cancer types, and glioblastomas (GBM and LGG) and uveal melanoma (UVM) rank the most significant worse outcome compared with other cancers (see Fig. 4d, the list of cancer abbreviations can be found in Supplementary Table S2). Extensive angiogenesis and markedly abnormal vessels are hallmarks of glioblastoma, characterized by hyperpermeability, resulting in tissue hypoxia. To determine pathological vascular, undergoing the EndoMT process; we examined the expression pattern of EMT marker Fibronectin and α-SMA in CD31-positive tumor vessels of human glioblastoma (grade IV glioma). The data show colocalization of the EMT marker in Figure 4e, indicating that the EndoMT occurs in tumor vasculature.

To investigate the mechanisms through which *FN1* regulates vascular function, the potential interacting proteins were analyzed using the Pearson correlation coefficient with the GMB dataset. We also included the VEGF pathway-related protein to determine its relation. It had identified that fibronectin interacts with the $\alpha 5\beta 1$ integrins, especially $\beta 1$ integrins,[25] and regulates VEGFR2 internalization[7] and FGFR1 phosphorylation.[26] The results show that ITGA5 and ITGA1 were significantly correlated with *FN1* (Figs. 4f, 4g), and the expression of VEGFR1, VEGFR2, and FGFR1 also correlated with *FN1* (Figs. 4h–j), but FGFR2, FGFR3, and VEGFR3 are not (Supplementary Fig. S5). When we investigated the VEGF pathway-related ligand, we found that VEGFA and VEGFB have no relation with *FN1* except VEGFB and VEGFD (Figs. 4k–n). This means that *FN1* regulates receptor activity and expression, affecting VEGFC and VEGFD expression.

Block Fibronectin Prevents VEGF Stimulator of Angiogenesis

To verify the role of *FN1* in angiogenesis, we use small interfering RNA (siRNA) on HUVEC. The efficiency of fibronectin silencing using siRNA was assessed through qPCR and Western blot analysis. Following siRNA transfection, a significant reduction in *FN1* mRNA and protein levels was observed compared with the control siRNA (Figs. 5a, 5b).

Silencing of fibronectin effectively mitigates the upregulation of p-VEGFR2 induced by VEGFA, except p-Akt and p-Erk (Fig. 5c). Furthermore, the scratch assay was performed to assess functional outcomes of migration. *FN1* siRNA-treated cells demonstrated diminished migratory capacity in response to VEGFA compared with the healthy control groups in HUVEC (Figs. 5d, 5e), continued with diminished fibronectin levels decreased VEGFA-induced cell proliferation with cell counting, a pivotal aspect of angiogenic response (Fig. 5f).

The results suggest that blocking fibronectin using siRNA impacts VEGFA-induced angiogenesis. These findings support the hypothesis that fibronectin plays a crucial role in

Investigative Ophthalmology & Visual Science

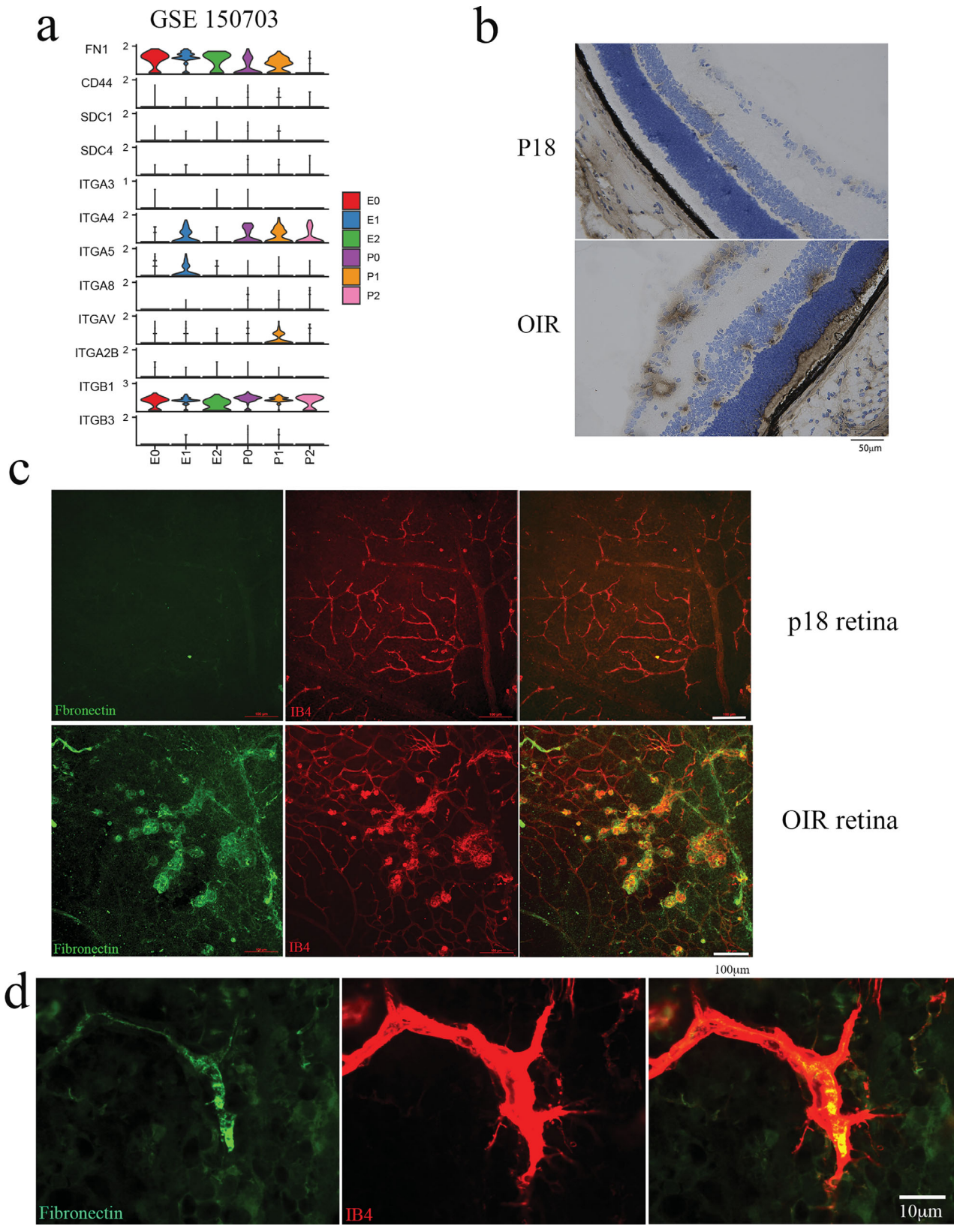

Figure 3. Fibronectin has upregulated in pathological vascular and tip cells in the OIR model. (**a**) Single cell sequence from GSE150703 shows the selected gene expression in a subtype of endothelial cell and pericyte in the OIR models. E0, E1, and E2 represent 3 subtypes of endothelial cells, and P0, P1, and P2 represent 3 subtypes of pericyte in the single cell sequence of GSE150703. (**b**) Immunohistochemical staining fibronectin in the retina section of p18 and OIR mouse model. Fibronectin (*brown*) was primarily confined in vascular-like tissue in the OIR retina section. (**c**) Immunofluorescence present fibronectin is expressed in pathological tufts vessels, co-staining of fibronectin (*green*) and IB4 (*red*) in the whole mount of OIR compared with normal vessels in p18 retina. (**d**) Fibronectin (*green*) was colocalized in the tip cell (*red*) of the OIR model.

Investigative Ophthalmology & Visual Science

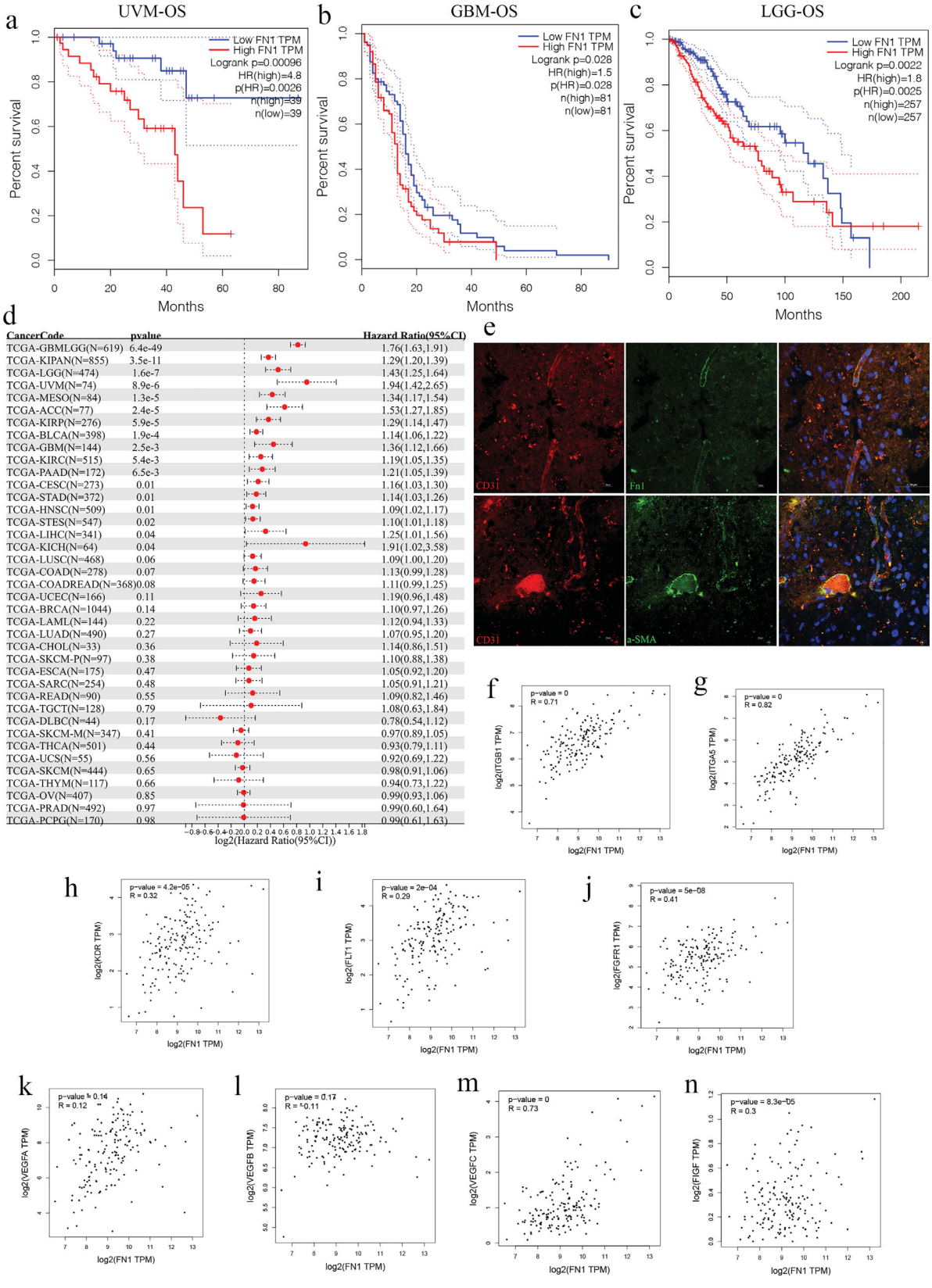

Figure 4. ***FN1* is a biomarker in GBM that correlates the FGF and VEGF pathways. (a–c)** Kaplan–Meier survival curve of patients with high and low expression of *FN1*, patients with low *FN1* expression (*blue line*) had significantly higher OS than those with high expression (*red line*) in TCGA-UMM, TCGA-GBM, and TCGA-LGG. **(d)** Forest plot of the effect of *FN1* on several cancers. Each *red point* represents the hazard ratio of *FN1* expression for the survival of cancers, and the *bars* around each point indicate the 95% confidence interval (CI). **(e)** Immunofluorescence present EMT marker is expressed in high-grade glioma vessels, co-staining of fibronectin or α-SMA (*green*) and CD31 (*red*) positive cells. **(f–n)** Shows the correlation analysis with Pearson correlation coefficient for *FN1* expression and different genes in the FGF and VEGF pathways by using the TCGA-GBM database.

Investigative Ophthalmology & Visual Science

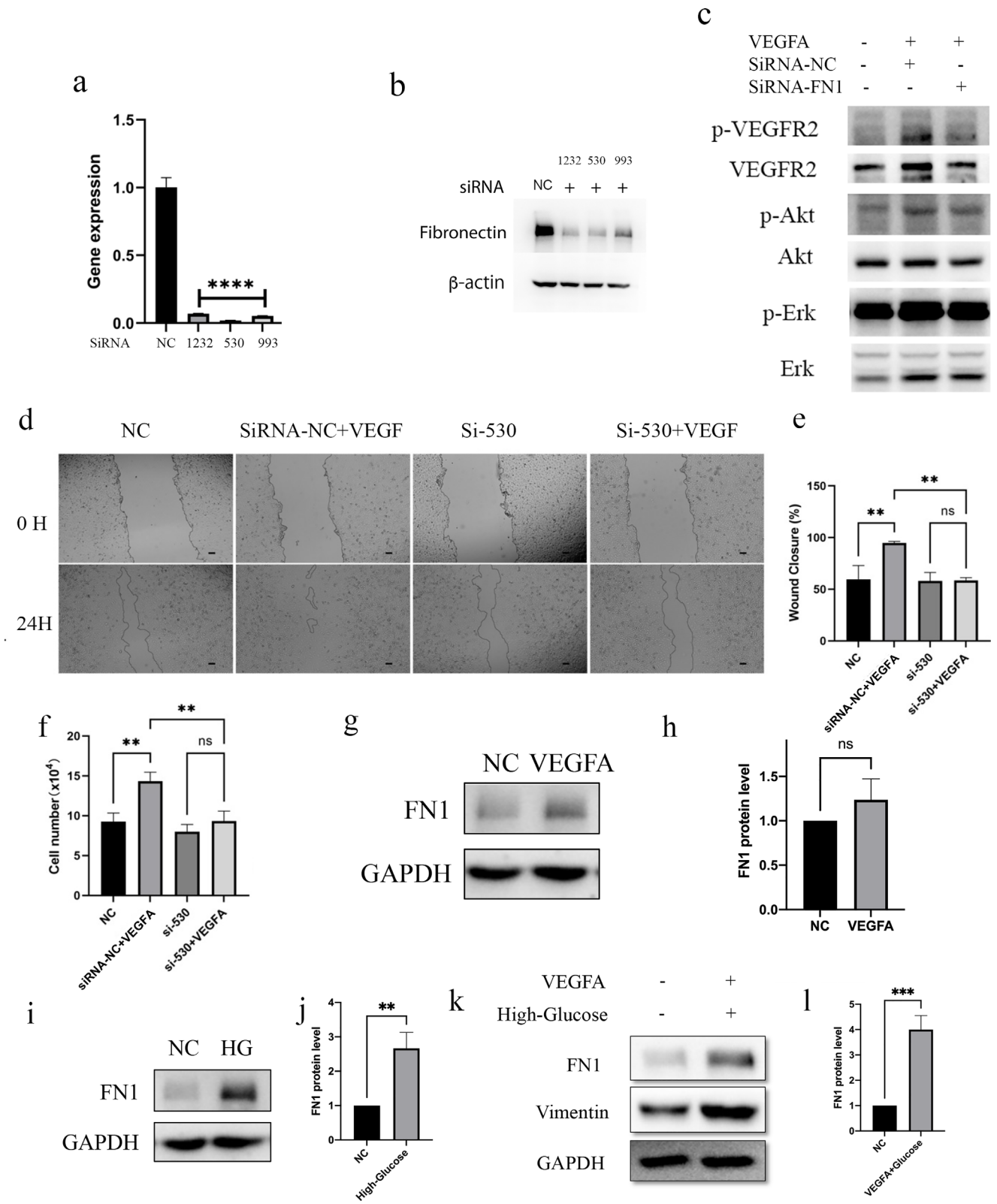

Figure 5. Silence Fibronectin prevents VEGFA-induced angiogenesis. (**a**) The mRNA level of the siRNA target *FN1* in HUVECs. The X-axis 1,232,993,530 represents 3 siRNA target *FN1* and the non-target control group (NC). (**b**) Western blot shows the protein expression using the siRNA target *FN1* and non-target control (NC), siRNA transfect to HUVECs for 48 hours and collect cell lysis for Western blot. (**c**) The results showed p-VEGF but not p-Akt, and p-Erk was prevented by *FN1* silence using siRNA 530, representing 3 independent experiments. (**d**) A wound was created by scraping the cell monolayer with a sterile pipette tip. The cells were treated with siRNA-530 (20 nM) or its vehicle, in addition to VEGFA (50 ng/mL). At 18 hours post-wounding, the wound was photographed under a microscope. Scale bar 50 mm. The data showed that silence fibronectin prevents VEGFA-induced cell migration. (**e**) Quantification of migration assay, representative of three independent experiments. (**f**) Proliferation tests by cell number counting, the cells were trypsin detached and then counted in a hemocytometer under a light microscope. The result showed that silence fibronectin prevents VEGFA-induced cell proliferation. (**g**) Western

blot for protein expression analysis. HRECs exposed to high VEGFA (50 ng/mL) for 24 hours were subjected to fibronectin expression analysis. (**h**) The intensity quantitation of protein expression was performed, (**i**) HRECs exposed to high D-glucose (50 mmol/L) for 24 hours were subjected to Western blot for protein expression analysis. The intensity quantitation of protein expression was performed in (**j**). (**k**) HRECs exposed to VEGFA (50 ng/mL) combined with high D-glucose (50 mmol/L) for 24 hours were subjected to Western blot for protein expression analysis. The intensity quantitation of protein expression was performed in (**l**). All Western blots had three independent experiments (folds). $^{**}P = 0.01$, $^{***}P = 0.001$.

regulating angiogenic processes, and its silencing may be a potential strategy for modulating pathological angiogenesis.

To mimic the retina microenvironment, we apply HRECs for further study on stimulation of fibronectin expression in DR conditions. Our findings have unveiled the elevation in fibronectin could not be induced by VEGF (50 ng/mL; Figs. 5g, 5h). In addition, we also found high glucose (50 mmol/L; Figs. 5i, 5j), or the conditions of high glucose and VEGFA are combined, a notably substantial approximately fourfold amplification in fibronectin expression within HRECs is witnessed (Figs. 5k, 5l). These results prove that fibronectin is upregulated and is not regulated by VEGFA.

Block *FN1* Prevents Growth Factor-Induced Proliferation and Migration

We had previously found the vitreous, which contains many factors, had a significant role in stimulating endothelial cell proliferation and migration during retina angiogenesis. Moreover, EGF and FGF might facilitate angiogenesis through a VEGF-independent pathway. Thus, we downregulates *FN1* by siRNA and see the role of *FN1* in different stimulator-induced endothelial cell proliferation and migration. Our investigations yielded outcomes that unequivocally showcased the efficacy of target *FN1* in countering vitreous, FGF, and EGF-induced cell proliferation with CCK8 assay (Figs. 6a–c), migration by scratch assay (Figs. 6d, 6f, 6h), and quantification shown in Figures 6e, 6g, and 6h.

Our observations showed that decreased fibronectin expression can prevent hypoxia and vitreous-induced cell response in retina angiogenesis. These findings underscore the pivotal role of fibronectin in disrupting retinal angiogenesis, which does not depend on VEGF activation.

Block *FN1* Alleviates Angiogenesis in OIR

To verify the influence of target *FN1* on angiogenesis within an in vivo context, we opted to use a mouse model of OIR. This model was selected because the preretinal tufts formed in this model closely mimic the pathological neovascularization characteristic of the human PDR.[5] We introduce siRNA (initial vitreal concentration of 1 µL 50 uM) or its corresponding vehicle (control siRNA, initial concentration of 0.1%) into the vitreous of mice at P12. Subsequently, the mice were reintroduced to room air conditions.

The group treated with *FN1* siRNA exhibited a striking reduction in preretinal tufts compared to the group receiving the vehicle injection (Fig. 7a). Remarkably, the administration of *FN1* siRNA not only curtailed fibronectin expression in vivo (Fig. 7b) but also exhibited a remarkable mitigation of other EMT markers such as E-cadherin, vimentin, and α-SMA (Fig. 7c). We found that the cell signaling of the EMT pathway represented by p-smad2/3 was also decreased in the retinas of mice subjected to *FN1* siRNA treatment (Fig. 7d). Quantification of these protein expressions is shown in Figure 7e. Taken together, these findings collectively point toward the effectiveness of downregulating *FN1* in impeding the process of EMT. These effects synergistically suppress pathological angiogenesis within a mouse model of OIR.

Discussion

DR poses a substantial global burden, resulting in considerable visual impairment.[4] The poor response to anti-VEGF treatment among patients with DR presents a therapeutic challenge. Our study reports that an aberrant increase in EMT signaling, especially EndoMT, starts with retina angiogenesis. The emergence of fibrosis during the late stages has an irreversible impact on neurons and vascular systems, leaving clinicians perplexed about the time needed for effective fibrosis prevention strategies. Based on our findings, the most significant GO enrichment of angiogenesis and extracellular matrix activity shows the intricate interplay between fibrosis and angiogenesis. We demonstrate that disruption of *FN1* by siRNA prevents VEGF-induced angiogenesis in vitro and in an OIR model. Therefore, our study reveals the therapeutics of early anti-fibrosis can inhibit neovascularization, especially the potential for non- or poor responders to anti-VEGF.

Angiogenesis and fibrosis are thought to be interdependent processes that often occur in parallel, with endothelial cell migration as a requisite for angiogenesis and fibrosis frequently gaining prominence in the initial stages of the disease.[27] Even a preclinical study of the PDR provides evidence that fibrosis can lead to a tractional retinal detachment and neurodegeneration, which cause severe vision loss in the end-stage of the disease[28–30]; we found EMT was started parallel with retina angiogenesis. Within our study, we observed a pronounced enrichment in angiogenesis and the extracellular matrix. Importantly, alterations in the EMT-related gene set, closely tied to angiogenesis, strongly indicate that these two interdependent processes take place in the early stages and can facilitate each other in hypoxia-induced retina angiogenesis.

Further reinforcement for the association between angiogenesis and fibrosis emerges from investigations conducted on liver fibrosis and certain cancer types. Experiments involving animal models have demonstrated that anti-angiogenic therapy can reduce fibrosis.[27,31] Moreover, our RNA-seq data corroborates the TGF-β signal's involvement, a pivotal EMT pathway, which closely intertwines with angiogenesis. This pathway is implicated in pathological processes tied to angiogenesis, and the emergence of potential therapeutics targeting the TGF-β pathway offers promise in curtailing diseases characterized by excessive angiogenesis.[32] Nevertheless, better comprehending the intricate relationship between fibrosis and angiogenesis remains crucial. This is because not all angiogenic targets hold therapeutic value, necessitating a refinement of therapeutic approaches toward anti-fibrosis targets that are more likely to yield beneficial outcomes. Given this complexity, targeting EMT might

Investigative Ophthalmology & Visual Science

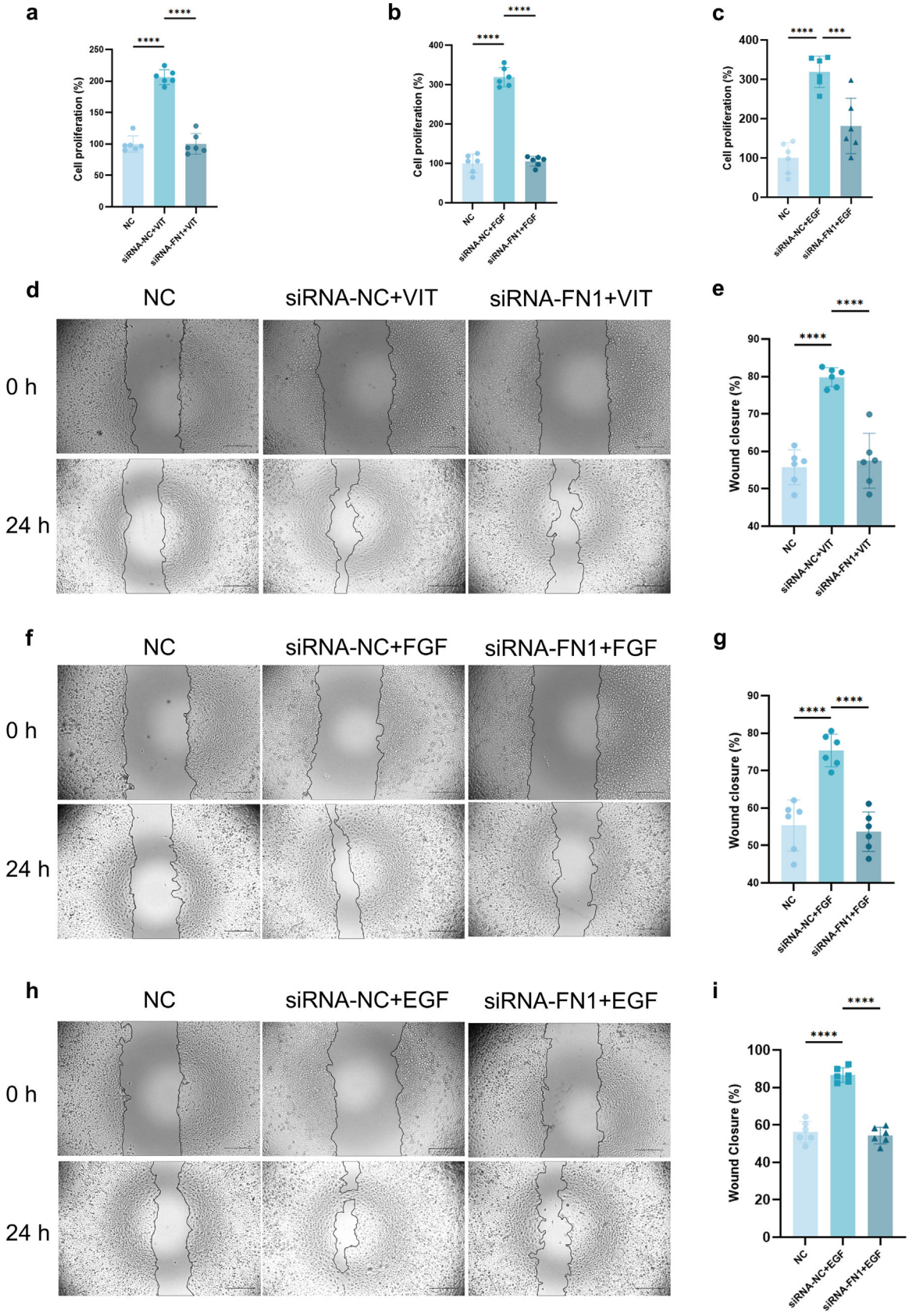

Figure 6. Effect of downregulated fibronectin on vitreous/FGF/EGF-induced cell proliferation and migration. **(a–c)** The inhibition of knockdown of fibronectin and negative control with vitreous/FGF/EGF on the proliferation of HUVEC cells was measured by CCK-8 assay ($n = 6$). ***$P < 0.001$; ****$P < 0.0001$. **(d, f, h)** Effects of knockdown of fibronectin and negative control on wound closure in HUVEC cells. Confluent cells were scratched and treated with vitreous/FGF/EGF. Light microscopic images of HUVEC cells were taken at 0 hours and 24 hours after the infliction of a scratch. Magnification = × 5. Scale bars = 100 µm. **(e, g, i)** Scratched areas were analyzed by ImageJ and GraphPad Prism ($n = 6$). ****$P < 0.0001$ versus the healthy control group.

Investigative Ophthalmology & Visual Science

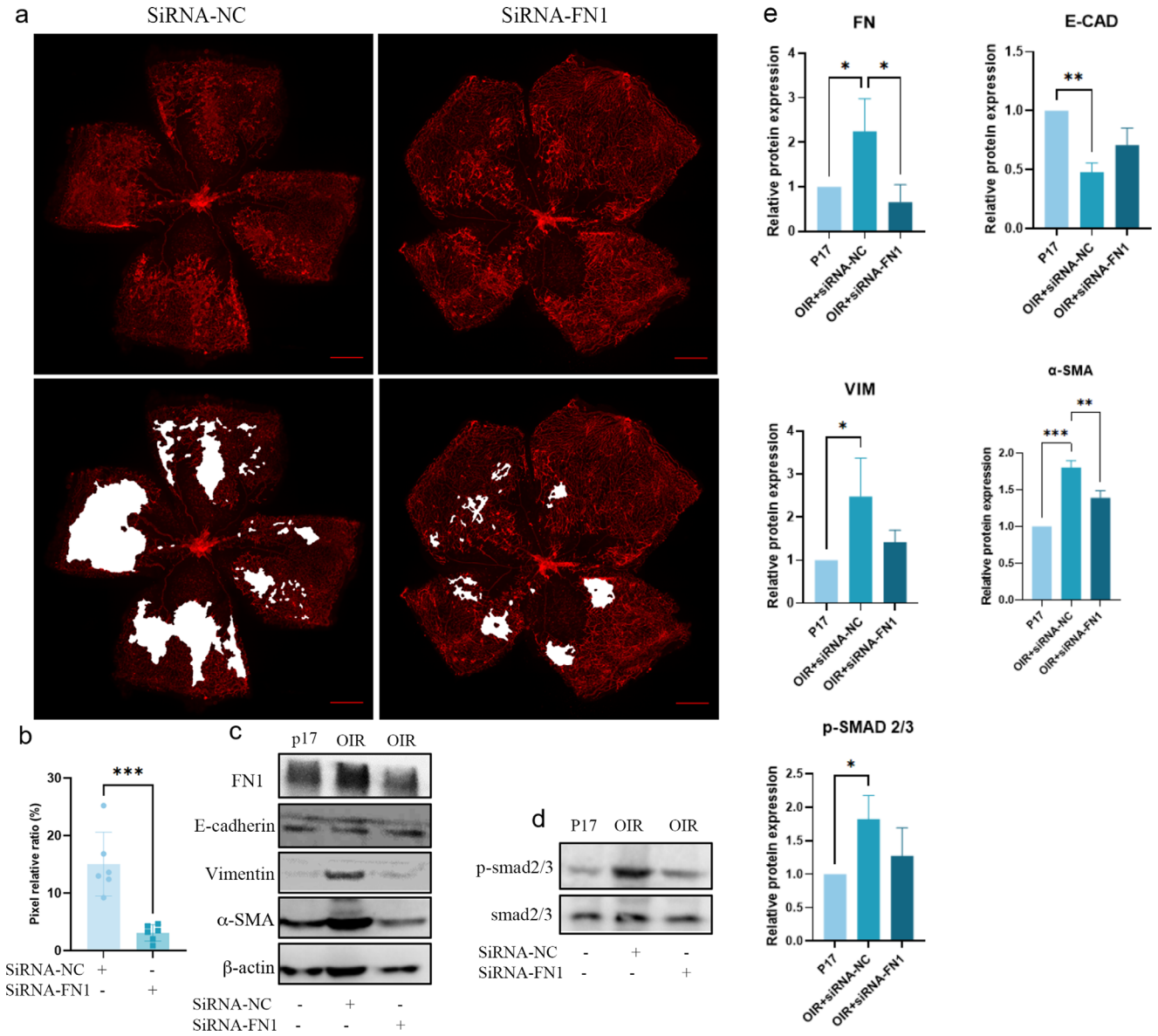

Figure 7. Downregulated fibronectin impedes pathological retinal angiogenesis in OIR. (a) P17 mice of OIR after intravitreal injection of *FN1* siRNA (*right*) or negative control siRNA into P12 OIR mice (*left*). At P17, the whole-mount retinas from the euthanized pups were stained with IB4. We outlined the tufts area with *white*. **(b)** Bar graphs were the data of IB4-stained retinas ($n = 6$) from mice intravitreally injected with negative control siRNA and *FN1* siRNA. At P17, the whole-mount retinas from the euthanized pups were stained with IB4. **(c)** Western blot analysis of protein from mouse retinas with antibody against Fibronectin, E-cadherin, Vimentin, and α-SMA after intravitreal injection of melatonin into P12 OIR mice ($n = 3$). **(d)** Western blot analysis of protein from mouse retinas with antibody against p-smad2/3 and smad2/3 between *FN1* siRNA administrated and healthy controls ($n = 3$). **(e)** Quantitation of protein expression.

offer a combined therapeutic approach to curbing angiogenesis and fibrosis in PDR or ROP.

Among these EMT genes, we found that *FN1* was the most significant gene increase in the OIR group, which is confirmed in other sequence data in GEO (see Fig. 2a). Subsequent exploration of localization shows that fibronectin is predominantly expressed in the vascular context (see Figs. 3c–d). This observation finds reinforcement in a study examining endothelial cells extracted from fibrovascular membranes of the PDR.[33] Furthermore, independent verification through single-cell sequencing reaffirmed the high expression of *FN1* within endothelial cells originating from the OIR retina.[34] Increasing *FN1* expression can be attributed to the sensitivity of these endothelial cells' exposure to hypoxic conditions. Signaling pathways, such as proliferation, angiogenesis, transformation, and apoptosis, were activated. In many in vivo and in vitro systems of sprouting angiogenesis, *FN1* is essential for tip cell migration.[35,36]

Additionally, fibronectin can bind VEGF or VEGFR2, a central regulator of angiogenesis, and directly influence it signaling output.[7,37,38] Notably, fibronectin can also disturb the FGF pathway.[39,40] In other endothelial disease model, endothelial cells exhibit EndoMT, which has been verified in pulmonary arterial hypertension[41–43] and systemic sclerosis.[44] In addition, much evidence underscores hypoxia as a trigger for EMT in various cancer types, such as breast cancer, prostate cancer, and oral cancer.[31,45,46] Our study verifies that during neovascularization and angiogenesis diseases, endothelial cells can undergo partial EndoMT

when generating new vascular cells. Thus, understanding the time of EndoMT in retinal angiogenic disorders needs further investigation.

In summary, these results shed light on the interconnectedness between EndoMT and angiogenesis, highlighting how retinal hypoxia sets in motion neovascularization and EndoMT concurrently. Our investigation pinpointed *FN1* as a possible biomarker and a mechanistic avenue implicated in angiogenesis. Despite the compelling evidence from our RNA-seq analysis demonstrating EMT involvement in OIR, several aspects require further investigation. The precise temporal dynamics of EMT during retinal angiogenesis, the complete spectrum of regulatory pathways beyond *FN1*, and validation in human retinal samples remain to be explored. Understanding these aspects will be crucial for developing targeted therapies for retinal neovascular diseases.

Acknowledgments

The authors thank the Department of Central Laboratory (Xiangya Hospital) and Huan Key Laboratory of Molecular Precision Medicine Laboratory (Central South University) for supporting this research.

Supported by a grant to W.W. from the National Natural Science Foundation of China (82271109 and 81900893) and the Science and Technology Plan Project of Hunan Province (2019RS2011) to W.W., and the Natural Science Foundation of Hunan Province (grant no. 2021JJ41030) to WW. Key Research and Development Foundation of Hunan Province: Application of retinal prosthesis in the treatment of advanced age-related macular degeneration (2020SK2119 to Q.Z), and Key Scientific Research Project of the Education Department of Hunan Province (23A0051 to Q.Z).

Author Contributions: W.W., D.L., L.P., and Z.W. performed the research and analyzed the data. F.C. and Z.M. performed the bioinformatic analysis. C.J. provided the clinical sample. Q.Z. conducted the immunohistochemical analysis for the sections of the eyes. W.W. designed the study, analyzed the data, and wrote the manuscript. J.L. revised the manuscript and performed project administration.

Ethics Approval and Consent to Participate: The Xiangya Hospital Ethics Committee reviewed and approved the study protocol (study title: study on the mechanism of PI3Kd mediate microglia activation in retina angiogenesis. Approval Number: 202310078 and Approval date: 2023.10.20). This study was conducted strictly according to the principles of the Declaration of Helsinki and local legislation. All participants were informed about the study's purpose, procedures, potential risks, and benefits.

Consent for Publication: All individual participants provided explicit consent to publish their data.

Availability of Data and Material: The datasets of several RNA sequences from other published papers can be obtained in GEO (GSE289223) and uncrop gel of WB was showing in supplement files.

Disclosure: **D. Liu**, None; **Z. Meng**, None; **C. Jin**, None; **F. Chen**, None; **L. Pu**, None; **Z. Wu**, None; **Q. Zeng**, None; **J. Luo**, None; **W. Wu**, None

References

1. Abu El-Asrar AM, De Hertogh G, van den Eynde K, et al. Myofibroblasts in proliferative diabetic retinopathy can originate from infiltrating fibrocytes and through endothelial-to-mesenchymal transition (EndoMT). *Exp Eye Res*. 2015;132:179–189.
2. Van Geest RJ, Lesnik-Oberstein SY, Tan HS, et al. A shift in the balance of vascular endothelial growth factor and connective tissue growth factor by bevacizumab causes the angiofibrotic switch in proliferative diabetic retinopathy. *Br J Ophthalmol*. 2012;96:587–590.
3. Hartnett ME, Penn JS. Mechanisms and management of retinopathy of prematurity. *N Engl J Med*. 2012;367:2515–2526.
4. Duh EJ, Sun JK, Stitt AW. Diabetic retinopathy: current understanding, mechanisms, and treatment strategies. *JCI Insight*. 2017;2:e93751.
5. Connor KM, Krah NM, Dennison RJ, et al. Quantification of oxygen-induced retinopathy in the mouse: a model of vessel loss, vessel regrowth and pathological angiogenesis. *Nat Protoc*. 2009;4:1565–1573.
6. Potts JR, Campbell ID. Fibronectin structure and assembly. *Curr Opin Cell Biol*. 1994;6:648–655.
7. Usuelli M, Meyer T, Mezzenga R, Mitsi M. VEGF and VEGFR2 bind to similar pH-sensitive sites on fibronectin, exposed by heparin-mediated conformational changes. *J Biol Chem*. 2021;296:100584.
8. Orr AW, Sanders JM, Bevard M, Coleman E, Sarembock IJ, Schwartz MA. The subendothelial extracellular matrix modulates NF-kappaB activation by flow: a potential role in atherosclerosis. *J Cell Biol*. 2005;169:191–202.
9. Yurdagul A, Jr., Green J, Albert P, McInnis MC, Mazar AP, Orr AW. $\alpha5\beta1$ integrin signaling mediates oxidized low-density lipoprotein-induced inflammation and early atherosclerosis. *Arterioscler Thromb Vasc Biol*. 2014;34:1362–1373.
10. Gelfand BD, Meller J, Pryor AW, et al. Hemodynamic activation of beta-catenin and T-cell-specific transcription factor signaling in vascular endothelium regulates fibronectin expression. *Arterioscler Thromb Vasc Biol*. 2011;31:1625–1633.
11. Lv Y, Xu WQ, Dong WG, et al. Integrin $\alpha5\beta1$ promotes BMCs mobilization and differentiation to exacerbate choroidal neovascularization. *Exp Eye Res*. 2020;193:107991.
12. Yin Y, Liu S, Liu H, Wu W. Nintedanib inhibits normal human vitreous-induced epithelial-mesenchymal transition in human retinal pigment epithelial cells. *Biomed Pharmacother*. 2023;166:115403.
13. Subramanian A, Tamayo P, Mootha VK, et al. Gene set enrichment analysis: a knowledge-based approach for interpreting genome-wide expression profiles. *Proc Natl Acad Sci USA*. 2005;102:15545–15550.
14. Hänzelmann S, Castelo R, Guinney J. GSVA: gene set variation analysis for microarray and RNA-seq data. *BMC Bioinformatics*. 2013;14:7.
15. Zou J, Tan W, Li B, et al. Interleukin-19 promotes retinal neovascularization in a mouse model of oxygen-induced retinopathy. *Invest Ophthalmol Vis Sci*. 2022;63:9.
16. Sun M, Wadehra M, Casero D, et al. Epithelial membrane protein 2 (EMP2) promotes VEGF-induced pathological neovascularization in murine oxygen-induced retinopathy. *Invest Ophthalmol Vis Sci*. 2020;61:3.
17. Binet F, Cagnone G, Crespo-Garcia S, et al. Neutrophil extracellular traps target senescent vasculature for tissue remodeling in retinopathy. *Science*. 2020;369:eaay5356.
18. Liu J, Lichtenberg T, Hoadley KA, et al. An integrated TCGA pan-cancer clinical data resource to drive high-quality survival outcome analytics. *Cell*. 2018;173:400–416.e411.
19. Liang CC, Park AY, Guan JL. In vitro scratch assay: a convenient and inexpensive method for analysis of cell migration in vitro. *Nat Protoc*. 2007;2:329–333.
20. Ruan GX, Kazlauskas A. Axl is essential for VEGF-A-dependent activation of PI3K/Akt. *EMBO J*. 2012;31:1692–1703.

21. Dieterich LC, Mellberg S, Langenkamp E, et al. Transcriptional profiling of human glioblastoma vessels indicates a key role of VEGF-A and TGFβ2 in vascular abnormalization. *J Pathol*. 2012;228:378–390.
22. Sun Y, Zhao C, Ye Y, et al. High expression of fibronectin 1 indicates poor prognosis in gastric cancer. *Oncol Lett*. 2020;19:93–102.
23. Kabir F, Apu MNH. Multi-omics analysis predicts fibronectin 1 as a prognostic biomarker in glioblastoma multiforme. *Genomics*. 2022;114:110378.
24. Tang Z, Li C, Kang B, Gao G, Li C, Zhang Z. GEPIA: a web server for cancer and normal gene expression profiling and interactive analyses. *Nucleic Acids Res*. 2017;45:W98–W102.
25. Al-Yafeai Z, Yurdagul A, Jr., Peretik JM, Alfaidi M, Murphy PA, Orr AW. Endothelial FN (fibronectin) deposition by α5β1 integrins drives atherogenic inflammation. *Arterioscler Thromb Vasc Biol*. 2018;38:2601–2614.
26. Zou L, Cao S, Kang N, Huebert RC, Shah VH. Fibronectin induces endothelial cell migration through β1 integrin and Src-dependent phosphorylation of fibroblast growth factor receptor-1 at tyrosines 653/654 and 766. *J Biol Chem*. 2012;287:7190–7202.
27. Huebert RC, Vasdev MM, Shergill U, et al. Aquaporin-1 facilitates angiogenic invasion in the pathological neovasculature that accompanies cirrhosis. *Hepatology*. 2010;52:238–248.
28. Zhang Q, Qi Y, Chen L, et al. The relationship between antivascular endothelial growth factor and fibrosis in proliferative retinopathy: clinical and laboratory evidence. *Br J Ophthalmol*. 2016;100:1443–1450.
29. Salzmann J, Limb GA, Khaw PT, et al. Matrix metalloproteinases and their natural inhibitors in fibrovascular membranes of proliferative diabetic retinopathy. *Br J Ophthalmol*. 2000;84:1091–1096.
30. Chou JC, Rollins SD, Ye M, Batlle D, Fawzi AA. Endothelin receptor-A antagonist attenuates retinal vascular and neuroretinal pathology in diabetic mice. *Invest Ophthalmol Vis Sci*. 2014;55:2516–2525.
31. Joseph JP, Harishankar MK, Pillai AA, Devi A. Hypoxia induced EMT: a review on the mechanism of tumor progression and metastasis in OSCC. *Oral Oncol*. 2018;80:23–32.
32. Zhu L, Lama S, Tu L, Dusting GJ, Wang JH, Liu GS. TAK1 signaling is a potential therapeutic target for pathological angiogenesis. *Angiogenesis*. 2021;24:453–470.
33. Lam JD, Oh DJ, Wong LL, et al. Identification of RUNX1 as a mediator of aberrant retinal angiogenesis. *Diabetes*. 2017;66:1950–1956.
34. Smith TL, Oubaha M, Cagnone G, et al. eNOS controls angiogenic sprouting and retinal neovascularization through the regulation of endothelial cell polarity. *Cell Mol Life Sci*. 2021;79:37.
35. Stenzel D, Lundkvist A, Sauvaget D, et al. Integrin-dependent and -independent functions of astrocytic fibronectin in retinal angiogenesis. *Development*. 2011;138:4451–4463.
36. Chiu CH, Chou CW, Takada S, Liu YW. Development and fibronectin signaling requirements of the zebrafish interrenal vessel. *PLoS One*. 2012;7:e43040.
37. Wijelath ES, Rahman S, Namekata M, et al. Heparin-II domain of fibronectin is a vascular endothelial growth factor-binding domain: enhancement of VEGF biological activity by a singular growth factor/matrix protein synergism. *Circ Res*. 2006;99:853–860.
38. Derricks KE, Trinkaus-Randall V, Nugent MA. Extracellular matrix stiffness modulates VEGF calcium signaling in endothelial cells: individual cell and population analysis. *Integr Biol (Camb)*. 2015;7:1011–1025.
39. Anderson AA, Kendal CE, Garcia-Maya M, et al. A peptide from the first fibronectin domain of NCAM acts as an inverse agonist and stimulates FGF receptor activation, neurite outgrowth and survival. *J Neurochem*. 2005;95:570–583.
40. Silva CA, Nardello LC, Garcia FW, et al. The role of FGF-2/HGF and fibronectin matrix on pleomorphic adenoma myoepithelial cell morphology and immunophenotype: an in vitro study. *Growth Factors*. 2015;33:50–56.
41. Cai D, Chen SY. Nanoparticle endothelial delivery of PGC-1α attenuates hypoxia-induced pulmonary hypertension by attenuating EndoMT-caused vascular wall remodeling. *Redox Biol*. 2022;58:102524.
42. Gorelova A, Berman M, Al Ghouleh I. Endothelial-to-mesenchymal transition in pulmonary arterial hypertension. *Antioxid Redox Signal*. 2021;34:891–914.
43. Ranchoux B, Antigny F, Rucker-Martin C, et al. Endothelial-to-mesenchymal transition in pulmonary hypertension. *Circulation*. 2015;131:1006–1018.
44. Li K, Wang Q, Bian B, Xu J, Bian H. Exploration and validation of the hub genes involved in hypoxia-induced endothelial-mesenchymal transition of systemic sclerosis. *Clin Exp Rheumatol*. 2023;41:1618–1631.
45. Harris AL. Hypoxia–a key regulatory factor in tumour growth. *Nat Rev Cancer*. 2002;2:38–47.
46. Heo K, Kim YH, Sung HJ, et al. Hypoxia-induced up-regulation of apelin is associated with a poor prognosis in oral squamous cell carcinoma patients. *Oral Oncol*. 2012;48:500–506.

Investigative Ophthalmology & Visual Science